

THERMALLY DRIVEN ATMOSPHERIC ESCAPE: TRANSITION FROM HYDRODYNAMIC TO JEANS ESCAPE

ALEXEY N. VOLKOV¹, ROBERT E. JOHNSON^{1,2}, ORENTHAL J. TUCKER¹, AND JUSTIN T. ERWIN¹

¹ Materials Science and Engineering Department, University of Virginia, Charlottesville, VA 22904-4745, USA

² Physics Department, New York University, NY 10003-6621, USA

Received 2010 October 1; accepted 2011 January 25; published 2011 February 16

ABSTRACT

Thermally driven escape from planetary atmospheres changes in nature from an organized outflow (hydrodynamic escape) to escape on a molecule-by-molecule basis (Jeans escape) with increasing Jeans parameter, λ , the ratio of the gravitational to thermal energy of the atmospheric molecules. This change is described here for the first time using the direct simulation Monte Carlo method. When heating is predominantly below the lower boundary of the simulation region, R_0 , and well below the exobase of a single-component atmosphere, the nature of the escape process changes over a surprisingly narrow range of Jeans parameters, λ_0 , evaluated at R_0 . For an atomic gas, the transition occurs over $\lambda_0 \sim 2-3$, where the lower bound, $\lambda_0 \sim 2.1$, corresponds to the upper limit for isentropic, supersonic outflow. For $\lambda_0 > 3$ escape occurs on a molecule-by-molecule basis and we show that, contrary to earlier suggestions, for $\lambda_0 > \sim 6$ the escape rate does not deviate significantly from the familiar Jeans rate. In a gas composed of diatomic molecules, the transition shifts to $\lambda_0 \sim 2.4-3.6$ and at $\lambda_0 > \sim 4$ the escape rate increases a few tens of percent over that for the monatomic gas. Scaling by the Jeans parameter and the Knudsen number, these results can be applied to thermally induced escape of the major species from solar and extrasolar planets.

Key words: hydrodynamics – planets and satellites: atmospheres – planets and satellites: individual (Pluto, Titan)

1. INTRODUCTION

Our understanding of atmospheric evolution is being enormously enhanced by extensive spacecraft and telescopic data on outer solar system bodies and exoplanets. The large amount of data on Titan's atmosphere from the *Cassini* spacecraft led to estimates of the atmospheric escape rate that, quite surprisingly, differed enormously (see Johnson 2009; Johnson et al. 2009). This was due to a lack of a kinetic model for how escape changes in character from evaporation on a molecule-by-molecule basis, referred to as Jeans escape, to an organized outflow, referred to as hydrodynamic escape, a process of particular interest to exoplanets (e.g., Yelle 2004; Murray-Clay et al. 2009) and to the early stages of atmospheric evolution (e.g., Watson et al. 1981; Hunten 1982; Tian et al. 2008).

Whether escape from a planet's atmosphere is hydrodynamic or Jeans-like is often characterized by the Jeans parameter, $\lambda = |U(r)|/(kT(r))$, where $U(r)$ is a molecule's gravitational energy at distance r from the planet's center, T is the temperature, and k is the Boltzmann constant (e.g., Chamberlain & Hunten 1987; Johnson et al. 2008). In Hunten (1982), it was suggested that if λ decreased to ~ 2 above the exobase, then the escape rate is not too different from the Jeans rate, but if λ became ~ 2 below the exobase, hydrodynamic escape would occur. Because the change in the nature of the escape process was assumed to occur over a *broad range* of λ , an intermediate model, the slow hydrodynamic escape (SHE) model, was adopted to describe the outflow from atmospheres such as Pluto's with exobase values $\lambda \sim 10$ (Hunten & Watson 1982; McNutt 1989; Krasnopolsky 1999; Tian & Toon 2005; Strobel 2008a). In the SHE model, based on Parker's (1964a, 1964b) model for the solar wind, the fluid equations, accounting for heat conduction, are solved to an altitude above which asymptotic conditions on the temperature and density are applied (e.g., Strobel 2008a). Other recent models couple the Jeans rate (Chassefiere 1996; Tian et al. 2008) or a modified Jeans rate (Yelle 2004; Tian 2009) to a continuum model. Although such approaches can give reasonable approximations, none can overcome a principal

drawback of fluid models: the application of near-equilibrium models to a part of the atmosphere, where the gas is rarefied and non-equilibrium effects are essential.

This Letter is aimed at revealing when the kinetic effects in atmospheric escape are important which we examine over a large range of λ including both hydrodynamic and Jeans escape. Such effects emerge due to the lack of translational equilibrium in an expanding gas and cannot be quantitatively predicted by familiar fluid models. To make clear when this is important for escape of the primary species, we use a kinetic model for a single-component atmosphere composed of a monatomic or diatomic gas.

2. DSMC SIMULATIONS

The transition from hydrodynamic to Jeans escape from planetary bodies is modeled here by the direct simulation Monte Carlo (DSMC) method (e.g., Bird 1994). It is a stochastic method for the numerical solution of flow based on the Boltzmann equation (e.g., Chapman & Cowling 1970). As in Parker's model, a spherically symmetric, single-component atmosphere is supplied by outgassing from a surface at radius R_0 . This can be the planet's actual surface with a vapor pressure determined by the solar insolation or a radial position in the atmosphere above which little heat is deposited and at which the density and temperature are known. In such a model, escape is driven by thermal conduction and heat flow from below R_0 . In the DSMC method, the gas is simulated by a large number of representative molecules of mass m . These molecules are subject to binary collisions and their trajectories are calculated in a gravity field: $U(r) = -GMm/r$, where M is the planet's mass and G is the gravitational constant. The mass of the gas above R_0 is assumed to be much smaller than M so that self-gravity is neglected.

The velocity distribution at $r = R_0$ is maintained to be Maxwellian for molecules with positive velocity component parallel to the local radial direction, $v_{\parallel} > 0$, at a fixed number density, n_0 , temperature, T_0 , and zero gas velocity. The exit

boundary at $r = R_1$ is placed far enough from R_0 so the flow above R_1 is approximately collisionless. A molecule crossing R_1 with v_{\parallel} and v_{\perp} will escape if velocity $v > (-2U(R_1)/m)^{1/2}$, where $v = \sqrt{v_{\parallel}^2 + v_{\perp}^2}$, while a molecule with a smaller v will return to R_1 with $-v_{\parallel}$ and v_{\perp} . R_1 is chosen to be sufficiently large to not affect the region described.

Although the principal results presented are for hard sphere (HS) collisions, comparisons made earlier using other models gave similar results (Tucker & Johnson 2009). It is readily shown that for a velocity-independent cross section, the Boltzmann equations, and, hence, the results presented here, can be scaled by two parameters: the *source* values of the Jeans parameter, λ_0 , and a Knudsen number, $Kn_0 = l_0/R_0$, where l_0 is the equilibrium mean free path of molecules at $r = R_0$. For HS collisions, $l_0 = (2^{1/2}n_0\sigma)^{-1}$, with σ being the collision cross section. The Knudsen number often discussed for a planet's atmosphere is $Kn(r) = l(r)/H(r)$, where $l(r)$ and $H(r)$ are the local mean free path and the atmospheric scale height, respectively. Since $Kn(R_0) = \lambda_0 Kn_0$, it can be used instead of Kn_0 . The simulations were carried out by fixing m , σ , T_0 , and R_0 with λ_0 and Kn_0 varied by changing M and n_0 . Since the results scale with λ_0 and Kn_0 , any two flows with different m , σ , T_0 , R_0 , M , and n_0 represent the same flow in dimensionless form if λ_0 and Kn_0 are the same. For comparison, we also model atmospheres composed of diatomic molecules with the collisions described by the variable hard sphere (VHS) model combined with the Larsen–Borgnakke (LB; e.g., Bird 1994) model, accounting for energy transfer between translational and internal degrees of freedom. A Maxwell–Boltzmann distribution of the energy of the internal degrees of freedom (Bird 1994) is assumed at $r = R_0$ for molecules with $v_{\parallel} > 0$. To represent low-temperature N_2 atmospheres, such as those at Pluto, Titan, and Triton, in the VHS-LB model the viscosity index is equal to 1 ($\sigma = \sigma_{\text{ref}} C_r/C_{r,\text{ref}}$, where C_r is the relative velocity of colliding molecules) and the number of internal degrees of freedom is 2 (Strobel 2008a, 2008b), and $l_0 = \sqrt{8kT_0/(\pi m)}/(n_0\sigma_{\text{ref}}C_{r,\text{ref}})$ (Bird 1994).

Simulations are initiated by “evaporation” from the cell at R_0 until steady flow is reached at large t . Steady state is assumed to occur when the number flux $4\pi r^2 n(r)u(r) = \Phi$ varies by less than $\sim 1\%$ across the domain, where $u(r)$ is the gas velocity and Φ is the escape rate. The independence of Φ on the simulation time was shown in test simulations, where the time before sampling the molecular parameters was sequentially increased by a factor of two, until no changes in Φ were found within accepted errors. Jeans escape, Φ_{Jeans} , is defined by the upward flux of molecules with velocities $v \geq (-2U(r)/m)^{1/2}$ at the nominal exobase, r_{exo} , determined by the scale height [$l(r_{\text{exo}}) = H(r_{\text{exo}})$] at large λ_0 or by the curvature [$l(r_{\text{exo}}) = r_{\text{exo}}$] at small λ_0 . Due to the limited number of simulation particles, accurately representing the tail of the velocity distribution is problematic at large λ_0 . In the solar system, λ_0 varies from ~ 0.01 for comets to ~ 10 for Pluto, and ~ 40 for Titan. For the test particle numbers used here, accurate escape rates are obtained for $\lambda_0 < 15$ which allows us to explore the transition region. For accurate escape rates, $R_1/R_0 = 40$ was required for $\lambda_0 \leq 10$; for $\lambda_0 > 10$, $R_1/R_0 = 6$ was sufficient. Gas parameters in Figure 1, which can be more sensitive to R_1 , are obtained using $R_1/R_0 = 100$.

3. RESULTS FOR THERMAL ESCAPE

A study was first carried out for HS collisions for $\lambda_0 = 0$ to 15 and a large range of Kn_0 . We focus here on small Kn_0 , so that the lower boundary is well into the collision-dominated

region of a planet's atmosphere where the fluid equations apply. Atmospheric properties versus r for a number of λ_0 with $Kn_0 = 0.001$ are shown in Figure 1. The dependence on r of the density, Mach number, and temperature are seen to be similar for small λ_0 (0, 1, 2), but, quite surprisingly, the radial dependence changes dramatically as λ_0 is increased (3, 10) with a distinct transition between 2 and 3. In particular, the number density n/n_0 and the ratio T_{\perp}/T_{\parallel} of perpendicular T_{\perp} and parallel T_{\parallel} temperatures at fixed r/R_0 tend to increase with increasing λ_0 for $\lambda_0 \leq 2$ and tend to decrease with increasing λ_0 for $\lambda_0 \geq 3$. The ratio, T_{\perp}/T_{\parallel} , considered a measure of translational non-equilibrium (Cattolica et al. 1974), remains close to unity in the transition region up to large r (e.g., up to $r/R_0 = 20$ for $\lambda_0 = 3$). Using the criteria in Cattolica et al. (1974), the onset of translational non-equilibrium for $\lambda_0 \leq 2$ is characterized by $l(r)/r \sim 0.05$. For $\lambda_0 \geq 3$ at $Kn_0 = 10^{-3}$, the transition to non-equilibrium is better characterized in terms of $Kn(r)$ with the onset of non-equilibrium increasing with increasing λ_0 , e.g., $Kn(r) \sim 0.1$ at $\lambda_0 = 3$ and $Kn(r) \sim 0.3$ at $\lambda_0 = 10$. Although T_{\perp} decays to zero, as expected at large r , it is seen in Figure 1(c) that T_{\parallel} does not go to zero.

More important to escape, the flow in Figure 1(b) is seen to be *hypersonic* for the small values of λ_0 , but, contrary to what has been assumed, it *never becomes hypersonic* for the larger λ_0 shown, even at very large r well above the exobase. At $\lambda_0 = 3$ the flow is seen to be *truly subsonic*. At $\lambda_0 = 10$, the flow velocity u does not exceed the *isentropic* sound speed $\sqrt{(5/3)kT/m}$ (here $T = (T_{\parallel} + 2T_{\perp})/3$). However, u can slightly exceed the isothermal sound speed, $\sqrt{kT/m}$, the critical velocity in Parker's (1964a) model. For example, for $\lambda_0 = 10$ and $Kn_0 = 10^{-2}$, $u = \sqrt{kT/m}$ at $r/R_0 \approx 80$. At $Kn_0 = 10^{-3}$ this does not occur until r/R_0 exceeds 100. At such distances, $l(r)/H(r) > 10^3$ so the flow is close to free molecular flow. If Kn_0 is increased, the flow approaches the free molecular limit and can become supersonic very far from the source at arbitrary λ_0 . But such flows cannot be quantitatively described using fluid models.

The properties at small Kn_0 for $\lambda_0 \leq 2$ roughly agree with those for an isentropic expansion above its sonic surface at $r = r_*$, where $u = \sqrt{(5/3)kT/m}$:

$$\begin{aligned} r^2 nu &= r_*^2 n_* u_*; \quad \frac{T}{n^{2/3}} = \frac{T_*}{n_*^{2/3}}; \quad \frac{5}{2}kT + \frac{mu^2}{2} - \frac{GMm}{r} \\ &= \frac{5}{2}kT_* + \frac{mu_*^2}{2} - \frac{GMm}{r_*}. \end{aligned} \quad (1)$$

In Equations (1), n_* , u_* , and T_* are evaluated at $r = r_*$. For small λ_0 and Kn_0 , r_* is located close to R_0 and hydrodynamic outflow occurs. As λ_0 increases to ~ 2 , the flow gradually decelerates (Figure 1(b)) and the thickness of the Knudsen layer decreases with decreasing Kn_0 : $r_* \rightarrow R_0$ (Figure 1(b)), and $T_* \rightarrow \sim 0.64T_0$ (Figure 1(c)). The latter is consistent with kinetic simulations of spherical expansion at zero gravity (e.g., Sone & Sugimoto 1993). Since $(5/2)kT_* + mu_*^2/2 - GMm/r_* \rightarrow 0$ as $\lambda_0 \rightarrow \sim 2.1$ a rapid deceleration of the flow occurs. Therefore, for the larger λ_0 , n/n_0 and T_{\parallel}/T_0 rise up to ~ 1 at R_0 , while the local Mach number rapidly drops below 0.1. At $\lambda_0 = 2-3$ and small Kn_0 , the rapid transition from hydrodynamic outflow to a nearly isothermal atmosphere below the exobase is such that above $\lambda_0 \sim 2.1$ the sonic point is *not reached* even at very large r and the atmosphere is gravitationally dominated. Therefore, the transition region is not broad at small Kn_0 and $\lambda_0 \sim 10$ is well above the region where escape by outflow occurs. This is unlike the prediction of Parker's (1964a, 1964b) model reformulated

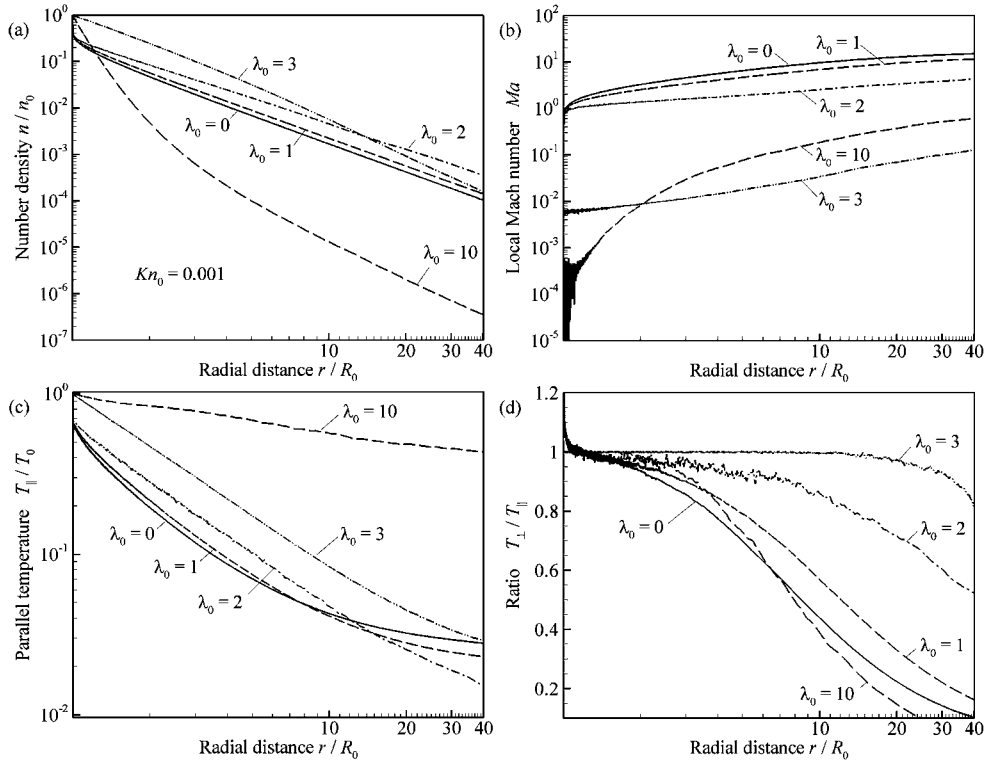


Figure 1. (a) Dimensionless properties: number density n/n_0 , (b) local Mach number $Ma = u/\sqrt{(5/3)kT/m}$, (c) T_{\parallel}/T_0 , (d) T_{\perp}/T_{\parallel} vs. r/R_0 for HS gas at $Kn_0 = 0.001$, $\lambda_0 = 0, 1, 2, 3, 10$. For $\lambda_0 \leq 2$ results are close to an isentropic expansion. Results fully scale with λ_0 and Kn_0 : simulations performed for fixed $m = 4.65 \times 10^{-26}$ kg, $\sigma = 7.1 \times 10^{-15}$ cm² (cross section for N₂ at 90 K; Bird 1994), $T_0 = 100$ K, $R_0 = 1000$ km, while M and n_0 were varied.

for an atomic gas, in which there is a critical point, beyond which supersonic expansion can occur, for every λ_0 .

Figure 2 shows the change in the parallel velocity distribution at $r/R_0 = 10$ for planets having different λ_0 . For $\lambda_0 \leq 2$, the distribution is shifted toward large v_{\parallel} and u is close to the most probable molecular velocity. For $\lambda_0 \geq 3$, the most probable v_{\parallel} is seen to be close to zero and escape is provided by the upward moving, high-speed molecules. This fact together with $T_{\perp} \neq T_{\parallel}$ highlights the non-equilibrium nature of the flow. In addition, for $\lambda_0 \geq 3$ the flow velocity and the molecular escape rate, Φ , cannot be associated with the maximum in the velocity distribution.

The effect of the change in the nature of the flow on Φ is shown in Figure 3. For the HS model, the ratio of Φ to the “evaporation” rate at R_0 , $\Phi_{0,0} = 4\pi R_0^2 n_0 \sqrt{kT_0}/(2\pi m)$ drops dramatically between $\lambda_0 = 2$ and 3 for both $Kn_0 = 0.001$ and 0.0003. Up to $\lambda_0 = 2$, the ratio is very close to ~ 0.82 , the rate found in the absence of gravity as in a comet-like expansion (e.g., Cong & Bird 1978; Crifo et al. 2002; Tenishev et al. 2008). The ~ 0.82 is due to collisions in the Knudsen layer causing the return flow. As the atmospheric outflow is choked off by the increased gravitational binding, $\Phi/\Phi_{0,0}$ rapidly drops a couple of orders of magnitude between $\lambda_0 = 2$ and 3. In this region, escape is a product of a rapidly decreasing fraction of the velocity distribution with $v > v_{\text{esc}}$ (Figure 2) and a rapidly decreasing flow velocity (Figure 1(b)). Therefore, for $\lambda_0 \geq 6$, it is seen that the escape rate is not very different from the Jeans rate contrary to what had been suggested. The ratio of Φ to the Jeans rate varies from 1.7 to 1.4 as λ_0 goes from 6 to 15, consistent with Tucker & Johnson (2009). A modified Jeans rate, accounting for the nonzero u , can provide an approximation to Φ at $\lambda_0 \leq 6$ (Volkov et al. 2011). At $\lambda_0 \geq 3$, values of $\Phi/\Phi_{0,0}$ even at $Kn_0 \sim 10^{-4}$ do not converge yet to values of the escape rate characteristic for the continuum limit, $Kn_0 \rightarrow 0$ (Figure 4).

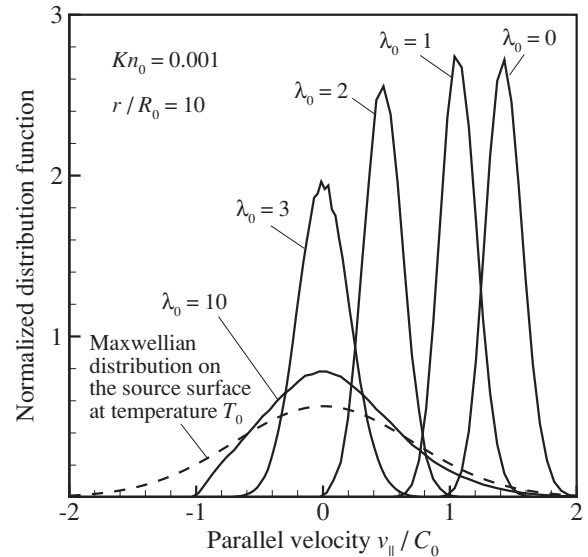


Figure 2. Normalized distributions of parallel velocity v_{\parallel}/C_0 in HS gas for $\lambda_0 = 0, 1, 2, 3, 10$ at $Kn_0 = 0.001$ and $r/R_0 = 10$. Black dashed curve: Maxwellian distribution at R_0 . $C_0 = \sqrt{2kT_0/m}$.

For comparison, the escape rate for an N₂ atmosphere calculated using the VHS-LB model is also shown in Figure 3 for $Kn_0 = 0.001$. The transition region remains narrow, shifting to $\lambda_0 \sim 2.4$ – 3.6 , but the lower limit, $\lambda_0 \sim 2.4$, still approximately corresponds to the upper limit for isentropic outflow for an N₂ atmosphere. For $\lambda_0 \sim 6$ – 15 , the escape rate for N₂ is $\sim 50\%$ – 15% larger than that for the HS gas due to the rotational–translational energy exchange. The rate is still only ~ 2.4 – 1.4 times the Jeans rate at the exobase for $\lambda_0 \sim 6$ – 15 , and not orders of magnitude

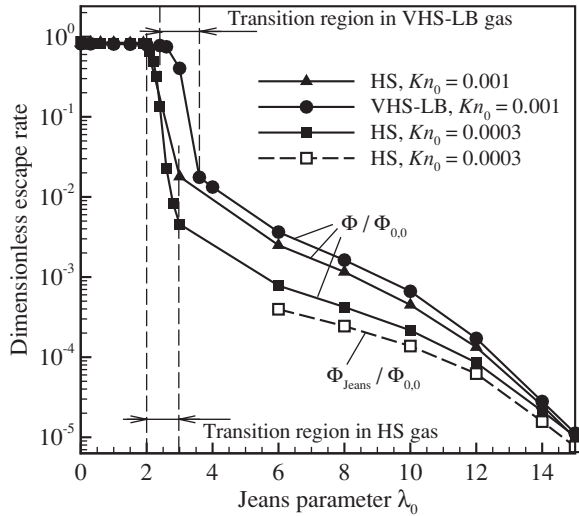


Figure 3. Dimensionless escape rate $\Phi/\Phi_{0,0}$ (solid curves) and Jeans escape rate $\Phi_{\text{Jeans}}/\Phi_{0,0}$ evaluated at the nominal exobase (dashed curve) vs. λ_0 at $Kn_0 = 0.001$ (circles and triangles) and $Kn_0 = 0.0003$ (squares). Square and triangles are for a gas composed of HS molecules; circle symbols: for a diatomic gas composed of VHS molecules with viscosity index equal to 1 and two internal degrees of freedom, described by the Larsen–Borgnacke (LB) model. $\Phi_{0,0} = 4\pi R_0^2 n_0 \sqrt{kT_0/(2\pi m)}$ is the evaporation rate on R_0 . Vertical lines indicate transition regions.

larger as predicted for N_2 at Pluto (Hunten & Watson 1982; McNutt 1989; Krasnopolsky 1999; Strobel 2008a) and Titan (Strobel 2008b).

In order to further test the fluid models, the heat flux calculated based on its kinetic definition (Bird 1994) is compared in Figure 5 to that in the fluid model for $\lambda_0 = 10$, a value relevant to Pluto and considered intermediate between cometary outflow and terrestrial atmospheres. It has been argued that at such λ_0 escape driven by thermal conduction can be continued into the exobase region (e.g., Strobel 2008b) a viewpoint criticized (Johnson 2010). It is seen that even a couple of scale heights below the exobase the heat flux is not well described by the Fourier law, $-\kappa(T)dT/dr$, where $\kappa(T)$ is the thermal conductivity for an HS gas (Chapman & Cowling 1970; Bird 1994). This law drastically overestimates the energy flux, consistent with $\lambda_0 = 10$ being well above the transition region. Thus, fluid models should be applied well below the exobase where the effects of translational non-equilibrium are negligible.

Our results can be used to evaluate calculations of loss rates for the principal atmospheric species. Although H_2 escape from Titan is significant, the large thermally induced loss rate estimated for the principal species is clearly incorrect, but plasma-induced escape can be important (Westlake et al. 2011) as predicted (Johnson et al. 2009). Simulations for trace species such as H_2 at Titan are in progress. For Pluto’s predominantly nitrogen atmosphere, when all of the heating is assumed to be below $R_0 = 1450$ km, the “zero heating case” ($Q = 0$) in Strobel (2008a) corresponds to $\lambda_0 \sim 23$. Therefore, the escape rate is close to the Jeans rate, giving a loss rate is orders of magnitude below that estimated ($\sim 5 \times 10^{28}$ amu s^{-1}). Of more interest is the loss rate for solar medium heating in Strobel (2008a). $Kn_0 = 0.01$ occurs at $R_0 \sim 3600$ km, which is well above the solar heating maximum and corresponds to $\lambda_0 \sim 10$. Using the results in Figure 4, the loss rate would be $\sim 7 \times 10^{27}$ amu s^{-1} , indicating that the energy limited value predicted ($\sim 9 \times 10^{28}$ amu s^{-1}) is inconsistent with the calculated atmospheric structure. Therefore, it is clear that modeling in support of the

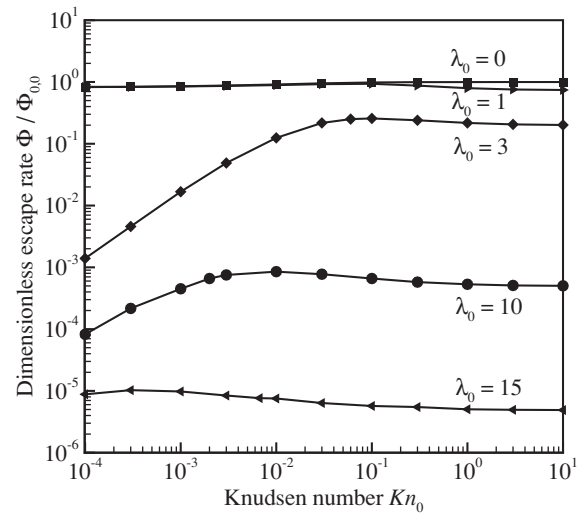


Figure 4. Dimensionless escape rate $\Phi/\Phi_{0,0}$ vs. Kn_0 at $\lambda_0 = 0, 1, 2, 3, 10$ for HS molecules.

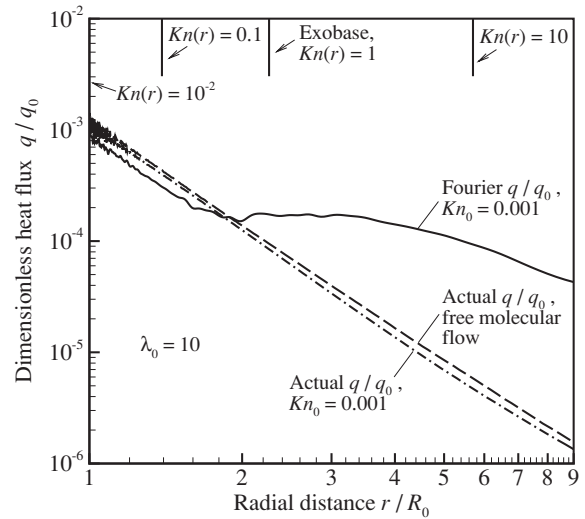


Figure 5. Dimensionless heat flux q/q_0 vs. r/R_0 for $\lambda_0 = 10$ in HS gas: $Kn_0 \rightarrow \infty$ (free molecular flow: dashed curve); $Kn_0 = 0.001$ (dash-dotted curve). Solid curve: dimensionless Fourier heat flux, $q = -\kappa(T)dT/dr$ calculated from $T(r)$ found in DSMC simulations at $Kn_0 = 0.001$ with thermal conductivity $\kappa(T)$ given by the first approximation of Chapman–Enskog for an HS gas (Chapman & Cowling 1970) and $q_0 = n_0 k T_0 \sqrt{2kT_0/m}$. Upper axis: $Kn(r) = l(r)/H(r)$.

New Horizon mission to Pluto will require a kinetic description of escape. Since the lower boundary occurs at a very small Knudsen number, a kinetic model of escape can be iteratively coupled to a fluid description of the lower atmosphere (Tucker et al. 2011). In a study of the EUV heating of Earth’s early atmosphere, Tian et al. (2008) found the onset of hydrodynamic escape of oxygen, and the resulting adiabatic cooling of the thermosphere, occurs at an exobase having a value of $\lambda \sim 5.3$. Since this is well above the heating peak and corresponds to a $Kn_0 \sim 0.2$, the inferred onset is in disagreement with the results presented here. As they used a modified Jeans rate, their escape rate is only a factor of ~ 4 too big. What is more important is the difference in the atmospheric structure near the exobase, which is dominated by non-equilibrium effects. Therefore, the fluid calculations of atmospheric escape from solar system bodies and exoplanets should be tested against kinetic simulations.

4. SUMMARY

A kinetic model was used to study the change in the nature of atmospheric escape from hydrodynamic to escape on a molecule-by-molecule basis. When heat is deposited primarily below the lower boundary of the simulation region, R_0 , and the collision cross sections are energy-independent, the results presented here can be *scaled* by two parameters evaluated at R_0 : The Jeans parameter, λ_0 , and the Knudsen number, Kn_0 (or $Kn(R_0)$). For R_0 in the collision dominated regime (small Kn_0) the transition from hydrodynamic to Jeans-like escape is found to occur over a surprisingly narrow range of λ_0 . Recently, Gruzinov (2011) showed that for $Kn_0 \rightarrow 0$ a hydrodynamic model of thermal escape, with appropriate boundary conditions, can give a sharp transition in escape rate. That is, below a critical value of λ_0 (~ 2.1 and ~ 2.4 for monatomic and diatomic gases), hydrodynamic outflow occurs and is roughly described by an isentropic expansion starting from the sonic surface. Above the transition regime (at $\lambda_0 > \sim 3$ and $\lambda_0 > \sim 3.6$ for monatomic and diatomic gases), escape occurs on a molecule-by-molecule basis. Depending on λ_0 , the fluid approximation for a monatomic gas breaks down when $Kn(r) < 0.1-0.3$ for $\lambda_0 = 3-10$, which is well below the exobase as seen in Figure 5. However, when a trace species is present, such as H_2 at Titan, the breakdown occurs at smaller $Kn(r)$.

For $\lambda_0 > \sim 6$ we show that the escape rates do not deviate enormously from the Jeans rate and we find only moderate differences between escape rates from monatomic and diatomic atmospheres. These results differ from what was predicted by Strobel (2008a, 2008b, 2009) based on a Parker-type (Parker 1964a, 1964b) model for a nitrogen atmosphere. Although our kinetic simulations are for a single-component, spherically symmetric atmosphere, the results have implications for complex atmospheres. Therefore, re-evaluation of studies for exoplanets, early terrestrial atmospheres, and the atmosphere of Pluto, soon to be visited by *New Horizon*, should be carried out using kinetic models of the upper atmosphere.

This work is supported by NASA's Planetary Atmospheres Program and the *Cassini* Data Analysis Program.

REFERENCES

- Bird, G. A. 1994, *Molecular Gas Dynamics and the Direct Simulation of Gas Flows* (Oxford: Clarendon), 218
- Cattolica, R., Robben, F., Talbot, L., & Willis, D. R. 1974, *Phys. Fluids*, **17**, 1793
- Chamberlain, J. W., & Hunten, D. 1987, *Theory of Planetary Atmosphere* (New York: Academic)
- Chapman, S., & Cowling, T. G. 1970, *The Mathematical Theory of Nonuniform Gases* (3rd ed.; Cambridge: Cambridge Univ. Press)
- Chassefiere, E. 1996, *Icarus*, **124**, 537
- Cong, T. T., & Bird, G. A. 1978, *Phys. Fluids*, **21**, 327
- Crifo, J. F., Loukianov, G. A., Rodionov, A. V., Khanlarov, G. O., & Zakharov, V. V. 2002, *Icarus*, **156**, 249
- Gruzinov, A. 2011, arXiv:1101.1103
- Hunten, D. M. 1982, *Planet Space Sci.*, **30**, 773
- Hunten, D. M., & Watson, A. J. 1982, *Icarus*, **51**, 655
- Johnson, R. E. 2009, *Phil. Trans. R. Soc. A*, **367**, 753
- Johnson, R. E. 2010, *ApJ*, **716**, 1573
- Johnson, R. E., et al. 2008, *Space Sci. Rev.*, **139**, 355
- Johnson, R. E., Tucker, O. J., Michael, M., Sittler, E. C., Waite, J. H., & Young, D. A. 2009, in *Titan from Cassini-Huygens*, ed. R. H. Brown et al. (Tucson, AZ: Univ. Arizona Press), 373
- Krasnopolsky, V. A. 1999, *J. Geophys. Res.*, **104**, 5955
- McNutt, R. L. 1989, *Geophys. Res. Lett.*, **16**, 1225
- Murray-Clay, R. A., Chiang, E. I., & Murray, N. 2009, *ApJ*, **693**, 23
- Parker, E. N. 1964a, *ApJ*, **139**, 72
- Parker, E. N. 1964b, *ApJ*, **139**, 93
- Sone, Y., & Sugimoto, H. 1993, *Phys. Fluids A*, **5**, 1491
- Strobel, D. F. 2008a, *Icarus*, **193**, 612
- Strobel, D. F. 2008b, *Icarus*, **193**, 588
- Strobel, D. F. 2009, *Icarus*, **202**, 632
- Tenishev, V., Combi, M., & Davidsson, B. 2008, *ApJ*, **685**, 659
- Tian, F. 2009, *ApJ*, **703**, 905
- Tian, F., Kasting, J. F., Liu, H.-L., & Roble, R. G. 2008, *Geophys. Res.*, **113**, E05008
- Tian, F., & Toon, O. B. 2005, *Geophys. Res. Lett.*, **32**, L18201
- Tucker, O. J., Erwin, J. T., Volkov, A. N., Cassidy, T. A., & Johnson, R. E. 2011, in *AIP Conf. Proc. 1333, 27th Int. Symp. on Rarefied Gas Dynamics* (Melville, NY: AIP), in press
- Tucker, O. J., & Johnson, R. E. 2009, *Planet Space Sci.*, **57**, 1889
- Volkov, A. N., Tucker, O. J., Erwin, J. T., & Johnson, R. E. 2011, *Phys. Fluids*, submitted
- Watson, A. J., Donahue, T. M., & Walker, J. C. G. 1981, *Icarus*, **48**, 150
- Westlake, J. H., Bell, J. M., Waite, J. H., Johnson, R. E., Luhmann, J. G., Mandt, K. E., Magee, B. A., & Rymer, A. M. 2011, *J. Geophys. Res.*, in press
- Yelle, R. V. 2004, *Icarus*, **170**, 167